Retraction Notice

The Editor-in-Chief and the publisher have retracted this article, which was submitted as part of a guest-edited special section. An investigation uncovered evidence of systematic manipulation of the publication process, including compromised peer review. The Editor and publisher no longer have confidence in the results and conclusions of the article.

Pin Wang agrees with the retraction. Peng Wang does not agree with the retraction. ZG, LZ, and HZ either did not respond or could not be reached.

Method of defogging unmanned aerial vehicle images based on intelligent manufacturing

Pin Wang,[a] Zhijian Gao,[b] Peng Wang,[c,*] Lingyu Zeng,[a] and Hongmei Zhong[a]

[a]Shenzhen Polytechnic, School of Mechanical and Electrical Engineering, Shenzhen, China
[b]Guangdong Key Laboratory of Intelligent Information Processing, Shenzhen Key Laboratory of Media Security, Shenzhen, China
[c]Kunming Institute of Botany, Chinese Academy of Sciences, Service Center for Information Technology, Kunming, China

Abstract. Intelligent manufacturing is a major trend in manufacturing innovation around the world, and it is also the main direction and key breakthrough point for the transformation and upgrading of the manufacturing industry for a long time now and in the future. Here, we mainly study the role of intelligent manufacturing in defogging unmanned aerial vehicle (UAV) images and how to analyze UAV image defogging methods based on intelligent manufacturing. In recent years, with the continuous progress of UAV technology, UAV project has also been booming. Aerial photographing is one of the most widely used functions of UAV at present. However, when photographing images in severe weather environment such as haze, it will be affected by the absorption and scattering of light by a variety of different suspended substances in the environment, resulting in poor imaging quality, color distortion, fine pitch blur, and other adverse effects. For this reason, there is a large amount of research on the image haze removal of UAV in China. At present, the mainstream methods are based on non-vision sensor and physical model. However, due to the lack of haze removal effect and severe condition limitation in the practical application of the above methods, we explore an innovative set of automatic estimation haze removal method of atmospheric light based on this method, taking the principle of atmospheric estimation direction as the main research direction, and then through the steps of setting the global transmittance, calculating the atmospheric light amplitude, adjusting the image size, and automatically modifying the image condition threshold value, etc. The man–machine image is haze removal. To compare the advantages and disadvantages of the three methods, we choose standard deviation, information entropy, and objective evaluation method to analyze the results of the three methods. Data analysis shows that among the three haze removal methods, the atmospheric light automatic estimation haze removal method has greatly improved the overall haze removal effect. Compared with the previous two kinds of haze removal imaging in the haze environment, it can better guarantee the color balance degree, and also retain more image information, which makes the imaging clarity have a significant improvement, and the overall effect is more natural. This method has played a very good complementary role to the domestic UAV demisting technology. [DOI: 10.1117/1.JEI.32.1.011216]

Keywords: image haze removal; atmospheric scattering; atmospheric light direction estimation; information entropy.

Paper 220300SS received Mar. 21, 2022; accepted for publication Aug. 10, 2022; published online Sep. 20, 2022.

1 Introduction

An unmanned aerial vehicle (UAV) is a kind of drone operated by radio control equipment and its own program. According to its different structure, it can be divided into fixed wing, parafoil, single rotor, multi rotor, etc. In recent years, UAVs have developed rapidly. Countries began to invest more people and resources in the research of UAVs. With the continuous improvement of

*Address all corrspondence to Peng Wang, wangpeng@mail.kib.ac.cn

1017-9909/2022/$28.00

technology level, UAV technology is more and more mature. In fact, it not only makes people carry out relevant research but also brings efficiency and convenience to people from all aspects. UAV is widely used in civil, military, and scientific research fields because of its small size, low cost, and simple structure. In civil field, it can be used for urban aerial photography, traffic monitoring, power detection, disaster monitoring, pesticide spraying, etc., and in the military aspect, UAV can carry out target monitoring, communication relay, air early warning, and military strikes.[1]

Intelligent manufacturing has gradually become the mainstream development model of global manufacturing. As an electronic tool that supports the deployment of resources and capabilities between manufacturing nodes, information systems play an active role in the digitization, networking, and intelligence of the manufacturing industry and are directly related to the overall competitive advantage of the intelligent manufacturing network. Specifically, information systems can not only meet the digital needs of manufacturing nodes characterized by computing, communication, and control applications but also can be networked connections to people, processes, data, and things, and can also sense, transmit, and store through the transformation of manufacturing nodes. The way of processing, presenting, applying, and inheriting data makes it possess the ability of learning, and finally enables manufacturing nodes to cooperate dynamically and respond to external demands faster and better.

At present, in good weather conditions, UAV obstacle recognition technology[2] has been relatively mature. But in the haze removal of complex environment, UAV still cannot work normally. In the complex haze removal environment, the existing UAV cannot independently perceive the surrounding environment information. Therefore, unknown obstacles may pose a threat to the UAV. Due to the continuous deterioration of the natural environment, the probability of the drone facing the environment such as smog will increase greatly. Therefore, the study of drone image smog removal has become an indispensable part of the drone research. A good study of haze removal will greatly improve the working capacity and application scope of existing UAVs.

Dehazing of UAV images has become an indispensable part of UAV research (atmospheric particles such as dehazing and haze can be called scattering phenomena, and are collectively referred to as dehazing for the convenience of description).[3,4] It uses some means to reduce or remove the interference of haze removal in the image so as to improve the image quality and visual effect and to obtain more effective image information. Image haze removal technology is an important branch of image processing. Because of its cutting-edge and wide application prospects, it has attracted people's attention and become a research hotspot in the field of image processing and computer vision. At present, according to whether it depends on the physical model of atmospheric scattering, the research of haze removal algorithm at home and abroad can be divided into two categories: one is based on non-visual sensors: ultrasound, radar, infrared, etc.; the other is based on nonphysical model. The main methods based on non-vision sensor are: (1) radar: radar uses electromagnetic wave to detect the target, sends the electromagnetic wave to the obstacle, receives its echo, and obtains the distance of the obstacle. There are many kinds of radars and various classification methods. According to the wavelength, it can be divided into millimeter wave, centimeter wave, decimeter wave, meter wave, etc. According to the location method, it can be divided into passive, active, and semi-active; and according to the purpose, it can be divided into meteorological, navigation, detection, and other types. The radar is not interfered by day and night, and can continuously detect the target all day; it has certain penetration ability and is not affected by rain and haze removal. Therefore, it is widely used in environmental perception and obstacle detection system.[5,6] (2) Ultrasound: the frequency of sound wave heard by human ear is between 20 and 20,000 Hz. Ultrasonic sensors usually convert ultrasonic signals into electrical signals, and calculate the distance information of the target according to the time interval. Ultrasound has the advantages of high frequency, good directivity, simple structure, and low cost. But the signal it sends out is sector area, which has a certain blind area. When multiple acoustic sensors work together, it is easy to receive the acoustic cross, resulting in the confusion of measurement data. (3) Infrared sensor: the infrared sensor is a sensor that uses infrared as the medium to complete the measurement. The principle is to measure the infrared receiving time and calculate the position information according to the formula. Wide measuring range and short response time. Small size, easy to install and operate; multi-sensor

Table 1 Methods, conclusions and limitations of this paper.

Items	Remarks			
The used techniques	Atmospheric light automatic estimation defogging method			
The findings	Simplifies the workflow	Increases the accuracy	Greatly improves the imaging effect	Complements the image defogging technique for UAVs well
The limitation of the proposed approaches	Although some results have been achieved, more work and experimental analysis is needed to support these results.			

synchronous measurement, long measurement distance. The above characteristics make the infrared sensor can be used in the research of UAV obstacle recognition.

Based on the scattering theory, a mathematical model of haze removal image degradation is established. Through the inversion of the formation process of haze removal image, a clear haze removal free image is obtained. According to the model, the image with haze removal consists of the reflected light of the object and the air light generated by the scattering of the haze removal particles suspended in the air, and the proportion of the reflected light is determined by the depth of field.[7,8] The process of image haze removal is the process of recovering the brightness of objects from the air light contained in the haze removal image. According to the different depth of field, there are two kinds of haze removal algorithms based on physical model. One is the algorithm assuming that the depth of the scene is known. Based on the known depth of field, a multi parameter statistical model is proposed to recover the haze removal image by estimating the scattering value and transmittance of pixels. The second is the algorithm based on multiple images. This algorithm can get the depth of field information from multiple photos of the same scene under different conditions and can achieve good haze removal effect. The limitation of the algorithm is to ensure that the shooting conditions are the same except for very limited factors such as weather conditions or polarization direction. This is often not easy or even impossible to achieve and will produce huge space and time costs, which also limits the application of such algorithms in production.[9,10]

Affected by the haze weather, the remote sensing image acquired by UAV in the measurement process always has different degrees of degradation. However, most of the existing haze removal algorithms for haze removal images are aimed at ordinary scene images, which are not completely suitable for the production of UAV images. For the aerial images taken by UAV, the flight height is usually several hundred meters or several thousand meters, and the difference of ground object height is almost negligible. Therefore, the obtained image depth of field can be regarded as a constant, and many assumptions of the existing methods are no longer valid. Therefore, according to the imaging characteristics of UAV in ground observation, this paper proposes an automatic atmospheric light estimation method. Taking the principle of atmospheric estimation direction as the main research direction, the UAV image is haze removal by setting the global transmittance, calculating the atmospheric light amplitude, adjusting the image size, and automatically modifying the image condition threshold and other steps. Compared with the existing image haze removal methods based on non-vision sensors and physical models, this method simplifies the workflow, improves the accuracy, improves the imaging effect greatly, and plays a good complementary role in the image haze removal technology of UAV.[11,12] Table 1 lists the limitations and inadequacies of the methods, conclusions, and methods used in this paper.

2 Unmanned Aerial Vehicle and Haze Removal Imaging Degradation

2.1 *Application and Development of Unmanned Aerial Vehicle*

UAVs are operated by radio control equipment and independent program control, or operated completely or intermittently by the onboard computer. With the rapid development of science and technology, UAV classification has obvious differences in use, speed, range, size, and other

Fig. 1 Consumer UAV.

aspects. Due to the increasing demand, there are more and more kinds of UAVs. According to the diversity of UAV, according to the platform configuration, it can be divided into the following three categories: fixed wing, multi-rotor, and unmanned helicopter.

It is divided into three categories: military, civil, and consumption. Military UAVs need intelligence, sensitivity, high speed, and the highest technical content, including reconnaissance, surveillance, communication relay, target aircraft, etc. Civil UAVs do not need high speed and range. Including traffic supervision, agriculture, meteorological monitoring, geological exploration, etc.; the cost of consumer UAV is relatively low, mainly used in aerial photography, competition, etc.[13] Figure 1 shows the more common consumer drones in real life.

In proportion: micro, small, light and large. The 7 kg of air mass is a micro UAV; the weight of a light UAV is between 8 and 120 kg, including 120 kg. The weight of the plane is 6000 kg, which is a small UAV. More than 6000 kg of aircraft are large UAVs.

The UAS is also called the unmanned aircraft system. At present, there are many kinds of UAVs in the market, but the system structure and composition are basically the same. The UAV system mainly consists of an aircraft, related remote control station, required command and control data link, and any other components specified by the model design. UAV has the characteristics of small size, light weight, flexibility, low cost, and has high application value. In the civil field, it is mainly used for aerial photography, urban traffic monitoring, meteorological observation, fire warning, etc. In the military field, it is mainly used for air reconnaissance, battlefield surveillance, communication, target tracking, and positioning, etc. The application of UAV greatly reduces human and intelligence, and greatly promotes the development of UAV itself as well as human production and life. Surveying and mapping, geological exploration, electronic warfare, and battlefield materials.[14,15]

2.2 *Mechanism of Image Degradation in Haze Removal*

1. Concept of haze: haze removal is an aerosol system composed of small water droplets or ice crystals formed by condensation of a large amount of water vapor suspended in the air near the surface. Small water droplets or ice crystals range in size from 1 to 100 μm, with an average diameter of 20 μm. They scatter roughly the same at all visible wavelengths, so haze removal usually looks milky white or blue white. The presence of haze removal reduces the transparency of the air and makes the horizontal visibility <1 km.

Haze is a common cloudy weather phenomenon, which is caused by a large number of dusts, sulfuric acid, nitric acid, organic hydrocarbons, and other very small non-aqueous aerosol particles floating in the air evenly. Dry dust particles range in size from 0.001 to 10 μm, with an average diameter of about 1 to 2 μm. Haze removal colors dark objects blue, and bright objects in the distance red and yellow. A large number of dry dust particles make the air turbid and the visibility is <10 km.

In meteorology, haze removal and haze are two different concepts, belonging to different weather phenomena. The thickness of haze removal is between tens of meters and 200 m, and the relative humidity is more than 90%. The thickness of haze is 1 to 3 km, and the relative humidity is <80%. In addition, the relative humidity in 80% to 90% of the weather phenomenon, known as haze. Haze is a new weather phenomenon in recent years. This is a mixed haze.[16,17]

2. Principle of atmospheric scattering: atmospheric optics research found that in sunny weather, the gap between air molecules is very large, and the reflected light from the field can enter the camera directly through the air molecules, without any negative impact on the scene image. However, in some special weather conditions, aerosol particles suspended in the air are easy to block and interfere with the reflected light in the scenic spot. When the specular reflected light is blocked and interfered by aerosol particles, it will produce scattering, absorption, and radiation. From the point of view of energy, scattering is a phenomenon that the energy carried by light in the atmosphere interacts with aerosol and other substances, and redistributes energy to all directions according to certain rules. It can cause changes in properties such as the color and intensity of light. For the same reason, light scattering from the sky, ground, water, and even other aerosol particles, floating in the air can also occur in the aerosol scattering, scattering can make other noise in addition to the reflection light from scenic spots enter the camera, and extra noise can make the reflected light enter the lens color and light intensity change characteristics. According to the size of the light wave length to the aerosol particle radius, the scattering can be divided into three categories: Raman Kraman scattering and Rayleigh scattering. When the particle diameter is >0.03 times of the wavelength, this kind of scattering is called meter scattering, and the scattering coefficient of meter scattering is independent of the wavelength of light.[18]

Haze is mainly due to the presence of some aerosol particles (including water-soluble and non-water-soluble) in the air, and the diameter of these aerosol particles roughly conforms to the Mikaelis scattering conditions. In this study, it is generally considered that in this case only Mikelis scattering occurs. Therefore, to restore the real scene of degraded image under the condition of haze weather, it is necessary to study the influence of Mahalanobis scattering on the image so as to clarify the physical process of image degradation. The following is an example of haze weather to illustrate the physical model of atmospheric scattering.

Attenuation model: the incident light attenuation model describes the phenomenon that the light emitted by the target scene is scattered by the suspended particles in the atmosphere before reaching the observation point so as to attenuate the light intensity at the observation point. The scattering medium in the air is simulated as a continuous medium. The incident light is considered as the change of the parallel light at α, $RE(\alpha,\kappa)$ is

$$RE(\alpha,\kappa) = -\beta(\kappa)E(\alpha,\kappa)R\alpha. \tag{1}$$

Among them, $\beta(\kappa)$ represents the scattering coefficient, which reflects the scattering ability of atmospheric medium to different wavelength beams. $RE(\alpha,\kappa)$ refers to the model for the attenuation of incident light. It is assumed that the atmospheric conditions are consistent over a short distance. By integrating Eq. (1) in $\alpha \in [0,R]$, d represents the scene depth:

$$E_a(r,\kappa) = E(0,\kappa)e^{-\beta(\kappa)r}. \tag{2}$$

The above formula $E_a(r,\kappa)$ represents the light intensity at the observation point, i.e., the result after attenuation. According to Eq. (2), the attenuation caused by atmospheric scattering is exponential with depth of field. It should be noted that the above equation is valid under the assumption that the incident light is a parallel light and the light intensity changes slowly. In the case of dynamic weather changes, the light intensity changes rapidly, so the above model is not correct. The research content of this paper is according to the above attenuation model in the case of single scattering.

Haze removal image degradation model: the attenuation model describes part of the light captured by the imaging device from the scene before entering the imaging device, after the absorption and scattering of suspended particles in the atmosphere. The ambient light model describes the imaging device part between the ambient atmospheric light entering the scene and the imaging device. According to the atmospheric scattering model proposed by McCartney, the haze removal image degradation model can be composed of the above two parts.[19] Therefore, the light intensity received by the imaging device can be expressed as

$$E(r,\kappa) = E_a(r,\kappa) + E_e(r,\kappa). \tag{3}$$

By taking Eq. (2) into the above formula to get

$$E(r,\kappa) = E_0(\kappa)e^{-\beta(\kappa)r} + E_\infty(\kappa)(1 - e^{-\beta(\kappa)r}). \tag{4}$$

In the above formula, $E_0(\kappa)e^{-\beta(\kappa)r}$ represents the incident light attenuation term, and $E_\infty(\kappa)(1 - e^{-\beta(\kappa)r})$ represents the ambient light interference term. By simplifying the above formula, the degradation model of haze removal image can be obtained as follows:

$$d(\alpha) = N(\alpha)t(\alpha) + B(1 - t(\alpha)), \tag{5}$$

where x represents the coordinates of the pixels in the image matrix; $d(\alpha)$ represents the haze removal image obtained by the imaging equipment; $N(\alpha)$ represents the radiation image in the haze removal free scene, i.e., the haze removal free image to be recovered by the atmospheric scattering model. B is the global atmospheric light, which is generally regarded as a constant; $t(\alpha) = e^{-\beta r(\alpha)}$ is the transmittance function, which reflects the ability of air to reflect light, where β is the atmospheric scattering coefficient, which can be regarded as a constant in a uniform medium and $R(\alpha)$ is the scene depth. From Eq. (5), we know that the purpose of demisting is to recover $N(\alpha)$ while the known quantity is only $I(x)$, which is a typical ill conditioned equation. Some prior knowledge is needed to estimate the transmissivity $t(x)$ and the global atmospheric light A so as to recover the haze removal free image $J(x)$.

3 Research Method

3.1 *Working Principle of Automatic Estimation of Atmospheric Light Direction*

Based on the physical model, the following models are often used to represent the haze removal image:

$$D(\alpha) = N(\alpha)t(\alpha) + B(1 - t(\alpha)), \tag{6}$$

where D is the haze removal image; N is the haze removal free image; B is the atmospheric light vector; t is the medium transmittance; and x is the location of the pixel.

For UAV imaging, it is mostly vertical or almost vertical downward. In this case, it can be considered that the medium transmissivity of each pixel in the UAV image is the same. The constant medium transmissivity is defined as the global transmissivity of the image, which is recorded as. Therefore, the UAV image haze removal model can be expressed as

$$D(\alpha) = N(\alpha)t_0 + B(1 - t_0). \tag{7}$$

By setting rules, several different albedo image blocks meeting the following equation can be automatically selected:

$$D(\alpha) = \iota'(\alpha)R_i t_0 + B(1 - t_0) = \iota(\alpha)R_i + B(1 - t_0). \tag{8}$$

Comparing Eqs. (7) and (8), it is evident that the haze removal free image $N(\alpha)$ is decomposed into $N(\alpha) = \iota'(\alpha)R_i$, where $\iota'(\alpha)$ is the scalar of the reflected light intensity and is the albedo vector of the first image block. The albedo of image block can be regarded as RGB vector of main color of image block.

Equation (3) combines $\iota'(\alpha)$ and t_0 into $\iota(\alpha)$, then, $N(\alpha) = \iota(\alpha)R_i$. It can be seen that the following haze removal free image block can be obtained by proper selection: most pixels on the image block are in the same straight line, and the direction of the straight line is the direction of the albedo vector R_i of the image block. Further analysis shows that the pixel points on the image block $D(\alpha)$ satisfying Eq. (8) are on the RGB plane formed by the albedo vector R_i and the atmospheric light vector A. This principle can estimate the direction of atmospheric light by selecting two or more image blocks from the images satisfying Eq. (8), that is, the direction

of atmospheric light vector A is the intersection line of RGB plane where two (or more) image blocks are located.[20,21]

3.2 *Principle of Atmospheric Optical Amplitude Estimation*

1. Global transmittance range: for general outdoor images, the corresponding transmittance of each pixel is

$$t(\alpha) = e^{-\beta d(\alpha)}, \tag{9}$$

where β is the atmospheric scattering coefficient and $R(\alpha)$ is the depth of field of pixel x.

For the UAV image, the atmospheric scattering coefficient β changes with the haze removal concentration. For a single UAV image with haze removal, β is difficult to estimate accurately. Because the depth of field $R(x)$ value is large and all pixels of the image are approximately equal, the global transmissivity t_0 is usually a fraction of the value close to 0, and some studies directly assume that the medium transmissivity of objects far away is 0.01. Without losing generality, the global transmittance of UAV image can be set to $t_0 = \varepsilon (0 < \varepsilon \leq 0.01)$.

2. Calculation of atmospheric light amplitude: write the atmospheric light vector B as the product $B = \vec{B}\|B\|$ of its direction $\vec{B}$ and amplitude $\|B\|$, Eq. (8) can be rewritten as

$$D(\alpha) = \iota(\alpha) R_i + \vec{B}\|B\|(1 - t_0). \tag{10}$$

It can be seen from Eq. (10) that the projection of the straight line of image block $D(\alpha)$ on vectors R_i and $\vec{B}$ is $\iota(\alpha)$ and $\|B\|(1 - t_0)$, respectively, whereas $\|B\|$ and $(1 - t_0)$ are fixed values. Therefore, we can draw the following conclusion: under ideal conditions, the image block satisfying Eq. (8) has the same projection in the direction of atmospheric light.

The above conclusion can be used to estimate the atmospheric light amplitude: according to the constraint conditions, select the pixel lines of P image blocks, calculate the projection amount of each pixel line on $\vec{B}$, find the average value of each projection value, and estimate the value of $\|B\|(1 - t_0)$, divide the average value by, and then calculate the atmospheric light amplitude $\|B\|$ (Fig. 2).

3.3 *Final Acquisition of Haze Removal Image*

The basic flow chart of this method is shown in Fig. 2. For a pair of haze removal image $D(\alpha)$, first use the above method to automatically select the image block, and then get the atmospheric light direction $\vec{B}$ according to the estimation principle of the atmospheric light direction; by setting the global transmittance t_0, use the atmospheric light amplitude calculation method to get the atmospheric light amplitude $\|B\|$; the final haze removal free image $N(\alpha)$ can be obtained by transforming Eq. (2):

$$\begin{cases} B = \vec{B}\|B\| \\ N(\alpha) = (D(\alpha) - B)/t_0 + B \end{cases}. \tag{11}$$

3.4 *Resize Image*

The key to select the image block satisfying Eq. (8) from the input image to estimate the direction $\vec{B}$ and amplitude of atmospheric light is as follows: according to the above constraints, the image block with negative surface albedo vector is excluded, and the included edge of the selected image block is avoided. To ensure this, we adopt the method of adaptive adjustment of image block size: first, select the image block size of 10×10 and judge that the number of image blocks satisfying the first two constraints is >100. If not, reduce the image block size to 9×9 for

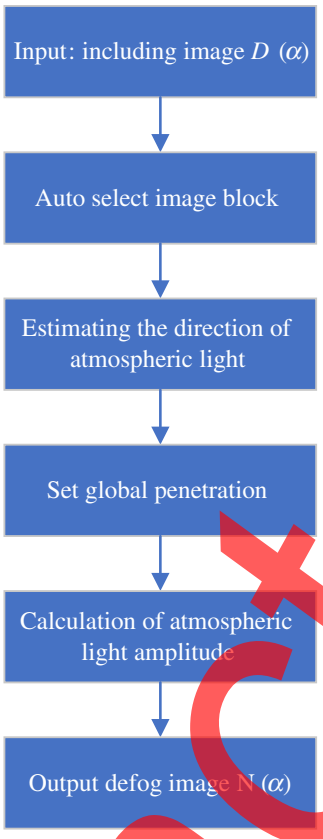

Fig. 2 Basic steps of this research method.

selection. If you choose to end, choose to terminate. When the number of reduced image blocks still does not exceed 100, continue to reduce the size of image blocks until the conditions are met. To ensure that there are enough pixels in the image block, set the minimum size of the image block to 5×5. If the requirements are not met, reduce the minimum size to 100 image blocks, the final number of image blocks shall prevail.[22,23]

3.5 *Adjust Image Condition Threshold*

To enhance the method, the adaptive method is used to adjust the thresholds ε_1, ε_2, and ε_3, and the specific steps are as follows:

The above 100 image blocks are sorted according to constraint 8 to constraint 10, and 50 image blocks are selected for each condition to form an image block reserve set, and the initial values ε_1, ε_2, and ε_3 are recorded.

The first 10 image blocks (i.e., $P = 10$) are sorted by extracting the threshold ε_1, ε_2, and ε_3 from a set of candidate image blocks. If the number of blocks is <10, the threshold ε_1, ε_2, and ε_3 will be reduced by 5% each time before the evaluation.

3. According to the 10 image blocks, calculate the line where the pixel is. The intersection point of 10 lines (the intersection point is averaged after two times) and the direction $\vec{B}$ of atmospheric light are unit vectors from the origin to the intersection point. About 10 image blocks are also used to estimate the intensity of atmospheric light $\|B\|$.[24]

3.6 *Image Quality Evaluation Method*

3.6.1 *Standard deviation*

Standard deviation (SD) is used to measure the contrast of an image, and its value directly reflects the amount of detail contained in the image. The larger the SD value of the image, the

richer the details from black to white, the higher the contrast, the better the color performance, and the better the quality of the detected image. On the contrary, the smaller the SD value is, the less the image details, the lower the contrast, the worse the color performance, and the worse the image quality.[25] The expression of SD is as follows:

$$\mathrm{SD} = \frac{1}{M \times N} \sum_{i=0}^{M-1} \sum_{j=0}^{N-1} \sqrt{(f(i,j) - \mu)^2}, \tag{12}$$

where $M \times N$ is the size of the image, $f(i,j)$ is the pixel value of the original input image, and μ is the average pixel gray value of the image.

3.6.2 *Information entropy*

Information hierarchy is a measure of the amount of information contained in an image. In the image, when the probability of each gray value is equal, the unit size is the largest. According to this theory, the larger the information entropy (IE), the more information the image contains. The smaller the IE value in the image, the less information it contains.[26] The expression is as follows:

$$IE[f(x,y)] = -\sum_{i=1}^{num} P_i \bullet \log_2 P_i. \tag{13}$$

In the above formula, n represents the gray level of the image, which is small and P_i represents the probability when the i'th gray-level appears.

3.6.3 *Objective evaluation index*

In the aspect of objective evaluation, the contrast and color fidelity of haze removal image are evaluated. Among them, the contrast evaluation index adopts the new visible edge ratio e. And the edge gradient before and after image blur is clearly visible $\overline{r}$. its expression is as follows:

$$\begin{cases} e = (n_r - n_0)/n_0 \\ \overline{r} = \overline{g}_r/\overline{g}_0 \end{cases}, \tag{14}$$

where n_0 and n_r in the haze removal free image and the s is the average gradient containing the dehazed free image, representing the number of visible edges; $\overline{g}_r$ is the average gradient of the s the average gradient of the haze removal containing image free image; $\overline{g}_0$ is the average gradient of the haze removal containing image.[27,28] Generally, e and $\overline{r}$ are large, and the edge intensity and number of the image increase after the surface is haze removal.

When evaluating the color fidelity of the haze removal image, this paper uses the hue fidelity as the evaluation index for measurement. The hue fidelity uses the measurement parameter H based on the image statistical characteristics proposed by Jobson et al., which represents the change of hue and is defined as

$$H = \mathrm{abs}\left(\frac{\mathrm{mean}(H_{\mathrm{out}}(x)) - \mathrm{mean}(H_{\mathrm{in}}(x))}{\mathrm{mean}(H_{\mathrm{in}}(x))}\right). \tag{15}$$

In the formula: $\mathrm{abs}(\cdot)$ means to take the absolute value of all elements; $\mathrm{mean}(\cdot)$ means to take the average value of all elements; $H_{\mathrm{in}}(x)$ and $H_{\mathrm{out}}(x)$ are the HSV space color image color composition before and after haze removal. Generally, the smaller the H value, the higher the color fidelity after haze removal.[29,30]

The article explains in order how to use intelligent manufacturing to dehaze UAV images. First, a physical model of the dehazing image is constructed, and then the dehazed image is finally collected based on the principle of atmospheric optical amplitude estimation, and finally adjusted. The size of the image, and the quality of the image is evaluated.

4 Experimental Results and Analysis

4.1 *Data*

To verify the atomization performance of the method in this paper, three UAVs flying to altitude of 1500, 3500, and 5500 m (under different weather conditions) were selected as the experimental image sources at different times in the haze removal environment, i.e., 512×500 dimension, 1392×1040, and 1392×1040.

4.2 *Analysis of Atmospheric Light Estimation Results*

To verify the influence of global transmittance setting on atmospheric light estimation, three groups of global transmittances t_0 were set to 0.015, 0.0055, and 0.0015, respectively (Table 2).

It can be seen from Fig. 3 that for the global transmittance in the range of (0, 0.015), the estimated atmospheric light direction is the same and the amplitude changes little. This indicates that the estimation results are more accurate. This is because the mean value of $\|B\|(1 - t_0)$ is used in the calculation of the atmospheric optical amplitude $\|B\|$. when $t_0 = \varepsilon(0 < \lambda \leq 0.01)$, $1 - t_0 \approx 1$ so $\|B\|(1 - t_0)$ can be approximately regarded as $\|B\|$. For the image taken by UAV at high altitude, generally t_0 can be set as a fixed value with a smaller value, such as $t_0 = 0.015$ in this experiment.

4.3 *Evaluation of Image Haze Removal Effect*

To evaluate the effectiveness of the method, three methods, subjective evaluation, objective evaluation and SD evaluation, are used to evaluate the effectiveness of the method. To facilitate

Table 2 Atmospheric light vector estimation results.

	Flight altitude 1500 m		Flight altitude 3500 m		Flight altitude 5500 m	
t_0	Direction	Range	Direction	Range	Direction	Range
0.015	(0.0836, 0.567, 0.5246)	320.46	(0.635, 0.6256, 0.5178)	416.32	(0.668, 0.5973, 0.4965)	393.16
0.0055		320.67		416.65		393.46
0.0015		320.87		416.98		393.79

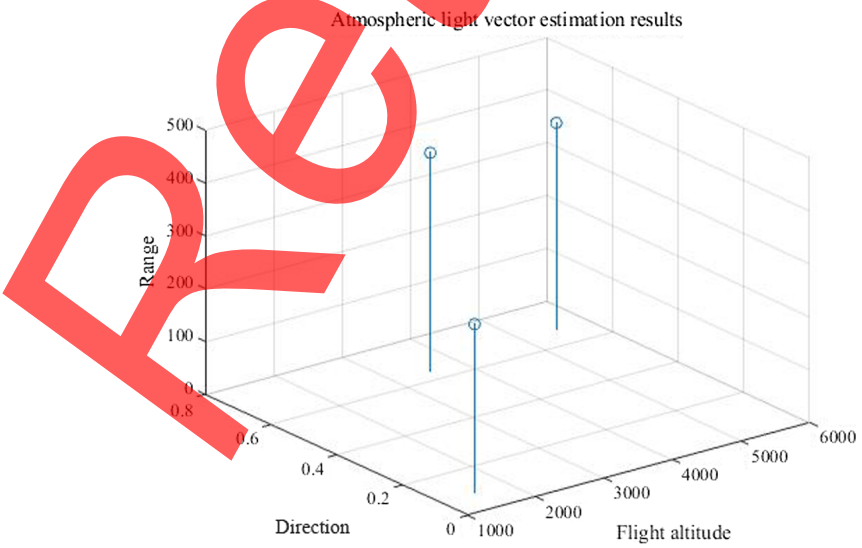

Fig. 3 Analysis chart of atmospheric light vector estimation results.

Fig. 4 Physical model demisting algorithm.

the comparison, we choose two classical haze removal methods (haze removal method based on non-vision sensor and haze removal algorithm based on physical model), and compare them with the existing methods. Dehazing based on physical model is more accurate to restore color. The experimental results are shown in Figs. 4 and 6.

4.3.1 *Subjective evaluation*

In terms of subjective evaluation, it can be seen from the haze removal effect in Fig. 4 that the physical model-based haze removal algorithm can improve the overall brightness but also cause the phenomenon of color distortion. Figure 5 shows a haze removal method based on non-vision sensor. As can be seen from the figure, the haze removal effect is generally dark, and the details in the distance are not obvious enough. Figure 6 is based on this chapter's atmospheric automatic estimation haze removal method, which realizes the effect clarity of non-vision sensor and improves the brightness at the same time.

Table 3 shows the quantitative evaluation results of three different methods after haze removal. We can conclude that compared with the other two methods, this method has the lowest e and $\bar{r}$ value and the highest H value. The results show that this method has strong texture detail protection and color fidelity; the method (based on non-vision sensor) is similar to the method in this paper in H value. The results show that the method has good color fidelity, but the e and $\bar{r}$ values are far behind the method in this paper. The quantitative index of the method (based on physical model) is the worst, the e and $\bar{r}$ values are low, and the H value is high. Compared with the above two methods, the quantitative indexes are not ideal.

4.3.2 *Standard deviation evaluation*

It can be seen from Fig. 7 that the SD test results of two haze removal methods (3) based on non-visual sensor (2) and physical model (3) are similar, but the atmospheric light automatic

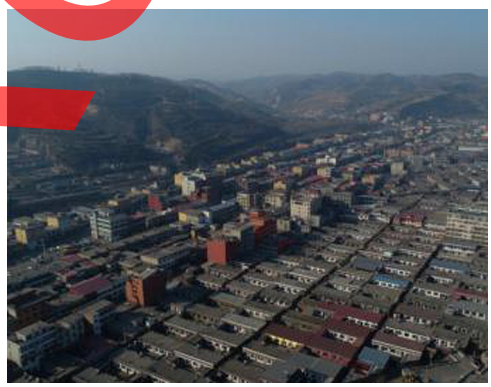

Fig. 5 Non-visual sensor approach.

Fig. 6 Atmospheric automatic estimation method.

Table 3 Quantitative evaluation results of three haze removal methods.

	Method based on non-vision sensor			Demisting algorithm based on physical model			Automatic estimation of atmospheric light		
Image source	e	$\bar{r}$	H	e	$\bar{r}$	H	e	$\bar{r}$	H
1	0.04	1.36	0.1356	0.05	1.42	0.0965	0.07	1.68	0.1235
2	0.05	1.58	0.0973	0.04	1.65	0.0792	0.09	2.45	0.0587
3	0.07	1.96	0.1175	0.08	1.69	0.063	0.12	2.98	0.0269

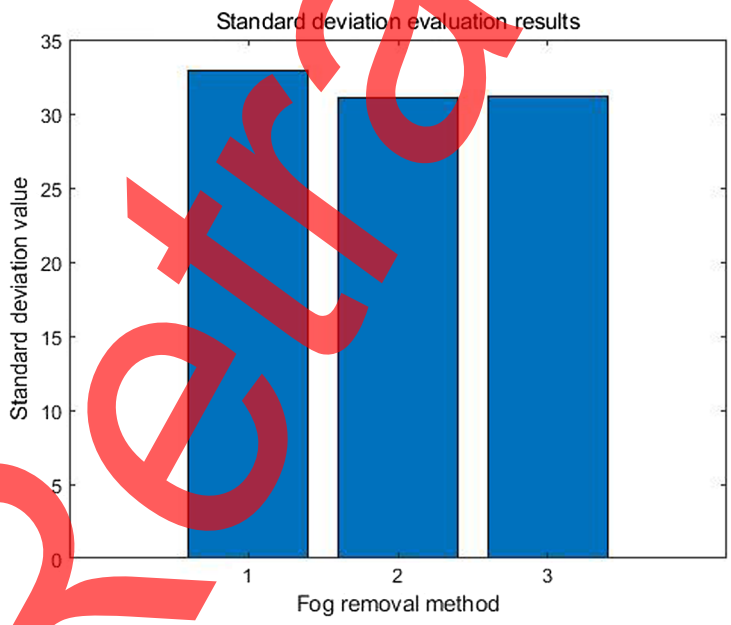

Fig. 7 SD evaluation results.

estimation method (1) adopted in this paper has been greatly improved, because it has a higher SD than the latter two. This shows that the automatic atmospheric light estimation method can retain more detailed information in the processing results, as well as better contrast and color performance. The comparative advantage of this method is that it can ensure good clarity when adjusting the color. Then we compare the execution time of these three methods, and the results are shown in Table 4 below.

Table 4 Execution time comparison.

Image source	Image size	Method based on non visual sensor	Defogging algorithm based on physical model	Automatic estimation of atmospheric light
1	320 × 480	40.861	24.873	8.886
2	232 × 345	22.864	13.6	4.336

5 Conclusions

UAVs have been widely used in real life with their unique advantages. In recent years, with the joint efforts of researchers, UAV-related technologies have made significant breakthroughs. Autonomous obstacle avoidance flight technology is becoming more and more mature, it can be divided into three stages, namely, the stage of perceiving obstacles, the stage of bypassing obstacles, and the stage of scene modeling and path searching, but in the haze removal and other harsh environment, the imaging effect of UAV will be greatly reduced. There are some natural conditions, as well as the development of software and hardware technology. To improve the application scope and utilization rate of UAV, and improve the ability of haze removal of UAV in haze environment, it has become a hot topic. Many researchers have made achievements in this field, and the actual effect has been verified and verified in practical application.

Intelligent manufacturing information system is an important information method to support the operation of intelligent manufacturing mode. Its robustness under the interference of internal and external environments is an important prerequisite and guarantee for the steady advancement of intelligent manufacturing and is a key scientific issue that needs to be broken in the process of intelligent manufacturing. It uses computers to simulate the intelligent activities of human experts to analyze, reason, judge, conceive and make decisions. It provides a solid foundation for UAV image defogging methods. Based on intelligent manufacturing, it is possible to better analyze and study the method of defogging UAV images. In this paper, the dehazing process of UAV images is carried out, and the problem of the slow dehazing speed of UAV images is initially solved, which provides examples and references for future dehazing of UAV aerial images.

This paper takes UAV to remove haze, target avoidance and target recognition as the research objects, designs related experimental models, and collects a large number of images and data information. Image noise reduction, haze removal, and haze removal optimization calculation method simplify the work style and improves the whole haze removal effect. Compared with the mainstream spray method of UAV (based on visual sensor method and haze removal algorithm based on physical model), we conclude that in this article, the author studies atmospheric automatic estimation to reduce haze removal effect, which can achieve good results while adjusting color. It is more natural than traditional methods to retain more image information and improve the clarity. This paper is a preliminary study of UAV spray. Although some results have been achieved, more work and experimental analysis are needed to support these results to improve the accuracy, real-time and authenticity of UAV imaging in haze environment. Next, we will study the in-depth comparison between our method and other methods so as to provide better ideas and methods for image dehazing. The constraint condition of the method in this paper is that the depth of field of the UAV images is similar, but this condition does not apply to the situation where the UAV performs imaging with a large oblique angle.

References

1. M. Mueller, N. Smith, and B. Ghanemm, "A benchmark and simulator for UAV tracking," *Far East J. Math. Sci.* **2**(2), 445–461 (2016).
2. R. X. Wei et al., "UAV guidance law for obstacle avoidance in unknown environment," *Xi Tong Gong Cheng Yu Dian Zi Ji Shu/Syst. Eng. Electron.* **37**(9), 2096–2101 (2015).
3. S. Mukhopadhyay and A. K. Tripathi, "Combating bad weather Part II: fog removal from image and video," in *Synthesis Lectures on Image Video and Multimedia Processing*, Vol. 8, No. 1, pp. 1–84 (2015).

4. C. B. Xiao et al., "Adaptive image fog removal based on multi-scale WLS filter," *J. Comput. Methods Sci. Eng.* **15**(1), 31–40 (2015).
5. Ş. Ulus and İ. Eski, "Neural network and fuzzy logic-based hybrid attitude controller designs of a fixed-wing UAV," *Neural Comput. Appl.* **33**, 8821–8843 (2021).
6. L. Zhang, D. Chen, and W. Liu, "Care robot indoor navigation method based on hybrid map," *Beijing Hangkong Hangtian Daxue Xuebao/J. Beijing Univ. Aeronaut. Astronaut.* **44**(5), 991–1000 (2018).
7. Y. Nan et al., "Evaluation of influences of frequency and amplitude on image degradation caused by satellite vibration," *Chin. Phys. B* **24**(5), 058702 (2015)
8. S. H. Bae and M. Kim, "DCT-QM: a DCT-based quality degradation metric for image quality optimization problems," *IEEE Trans. Image Process.* **25**(10), 4916–4930 (2016).
9. H. Zhao et al., "Target detection over the diurnal cycle using a multispectral infrared sensor," *Sensors* **17**(1), 56 (2016).
10. J. Wang et al., "Single image dehazing based on the physical model and MSRCR algorithm," *IEEE Trans. Circuits Syst. Video Technol.* **28**(9), 2190–2199 (2017).
11. Y. Wang et al., "Adaptive sampling for UAV tracking," *Neural Comput. Appl.* **32**, 5029–5043 (2019).
12. L. Shu-Jun, "The practice and exploration of unmanned aerial vehicle (UAV) three dimensional tilt photography technology in monitoring open pit mines," *World Nonferrous Metals* (7), 194–194 (2019).
13. C. Thiel and C. Schmullius, "Comparison of UAV photograph-based and airborne lidar-based point clouds over forest from a forestry application perspective," *Int. J. Remote Sens.* **38**(8), 1–16 (2016).
14. Y. Khosiawan and I. Nielsen, "A system of UAV application in indoor environment," *Prod. Manuf. Res.* **4**(1), 2–22 (2016).
15. C. Eling et al., "Development and evaluation of a UAV based mapping system for remote sensing and surveying applications," *Int. Arch. Photogramm. Remote Sens. Spatial Inf. Sci.* **XL-1/W4**, 233–239 (2015).
16. J. J. Zhang and J. M. Samet, "Chinese haze versus Western smog: lessons learned," *J. Thorac. Dis.* **7**(1), 3–13 (2015).
17. W. J. Yi et al., "Restoration of longitudinal laser tomography target image from inhomogeneous medium degradation under common conditions," *Opt. Express* **25**(14), 15687–15698 (2017).
18. J. Yang et al., "A RGB channel operation for removal of the difference of atmospheric scattering and its application on total sky cloud detection," *Atmos. Meas. Tech.* **10**, 1191–1201 (2016).
19. J. U. Ming-Ye and Z. Deng-Yin, "Image enhancement based on prior knowledge and atmospheric scattering model," *Acta Electron. Sin.* **45**(5), 1218–1225 (2017).
20. T. Narihira, M. Maire, and S. X. Yu, "Direct intrinsics: learning albedo-shading decomposition by convolutional regression," in *Int. Conf. Comput. Sci.*, pp. 2992–2992 (2015).
21. Z. Tang, X. Zhang, and W. Lan, "Efficient image encryption with block shuffling and chaotic map," *Multimedia Tools Appl.* **74**(15), 5429–5448 (2015).
22. I. Perfilieva et al., "Image reduction method based on the F-transform," *Soft Comput.* **21**, 1847–1861 (2015).
23. J. M. Guo, H. Prasetyo, and J. H. Chen, "Content-based image retrieval using error diffusion block truncation coding features," *IEEE Trans. Circuits Syst. Video Technol.* **25**(3), 466–481 (2015).
24. L. C. Chen et al., "DeepLab: semantic image segmentation with deep convolutional nets, atrous convolution, and fully connected CRFs," *IEEE Trans. Pattern Anal. Mach. Intell.* **40**(4), 834 (2018).
25. S. Tang and A. B. Yeh, "Approximate confidence intervals for the log-normal standard deviation," *Quality Reliab. Eng. Int.* **32**(2), 715–725 (2016).
26. R. Zhou et al., "A portfolio optimization model based on information entropy and fuzzy time series," *Fuzzy Optim. Decis. Making* **14**(4), 381–397 (2015).
27. Y. Bai et al., "Real-time instruction-level verification of remote IoT/CPS devices via side channels," *Discov. Internet Things* **2**, 1 (2022).

28. Z. Yu et al., "Fusion method of optical image and SAR based on UAV," *J. Appl. Opt.* **38**(2), 174–179 (2017).
29. D. J. Bora, "A novel approach for color image edge detection using multidirectional Sobel filter on HSV color space," *Int. J. Comput. Eng.* **5**(2), 154–159 (2017).
30. S. Zhu et al., "Cross-space distortion directed color image compression," *IEEE Trans. Multimedia* **20**(3), 525–538 (2018).

Pin Wang received her PhD from Shenzhen University, P.R. China, in 2012. Now, she is a teacher at Shenzhen Polytechnic. Her research interests include cloud data fusion, signal processing, and multi-target tracking.

Zhijian Gao obtained his master's degree in electronics and information engineering from Shenzhen University in 2012. Now, he is working at the School of Electronics and Information Engineering, Shenzhen University. His research interests include machine vision and sensor network.

Peng Wang received his master's degree from Zhongnan University of Economics and Law, P.R. China, in 2018. Now, he is a staff of Service Center for Information Technology, Kunming Institute of Botany, Chinese Academy of Sciences.

Lingyu Zeng received his PhD from Sun Yat-sen University, P.R. China, in 2019. Now, he is a teacher at Shenzhen Polytechnic. His research interests include optical properties in micro-nano structures, quantum optics, and biophysics.

Hongmei Zhong received her PhD from City University of Hong Kong, P.R. China, in 2021. Now, she is a teacher at Shenzhen Polytechnic. Her research interests include renewable energy, signal processing, and thermal management.